Environmental Toxicology and Pharmacology 104 (2023) 104310

Contents lists available at ScienceDirect

Environmental Toxicology and Pharmacology

journal homepage: www.elsevier.com/locate/etap

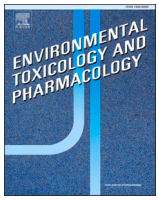

Cytotoxicity, morphological and ultrastructural effects induced by the neonicotinoid pesticide, imidacloprid, using a rat Leydig cell line (LC-540)

MIA Ibrahim *, GCH Ferreira, EA Venter, CJ Botha

Department of Paraclinical Sciences, Faculty of Veterinary Science, University of Pretoria, Onderstepoort 0110, South Africa

ARTICLE INFO

Keywords:
Autophagy
Cytoskeletal proteins
Cytotoxicity
Imidacloprid
Leydig cell line (LC-540)
Mitochondria
Neonicotinoid

ABSTRACT

Imidacloprid is a systemic neonicotinoid insecticide widely used to combat agricultural pests and flea infestations in dogs and cats. Despite its low toxicity to mammals, imidacloprid is reported to cause male reproductive toxicity. This study evaluated the cytotoxic effects of 75–800 μM imidacloprid on a rat Leydig cell line (LC-540). The effect of exposure to 300, 400, and 500 μM imidacloprid on selected cytoskeletal proteins, mitochondrial morphology, lysosomal acidity, and ultrastructure were investigated. Cell viability was markedly reduced after 48 and 72 h of exposure to higher imidacloprid concentrations. The immunocytochemical analysis revealed that the cytoskeletal filaments exhibited disorganization, disruption, and perinuclear aggregation in treated LC-540 cells. Ultrastructurally, cytoplasmic vacuoles, autophagic vacuoles, lysosomes, and mitochondrial damage were detected. Changes in the mitochondrial morphology and lysosomes induced by imidacloprid were confirmed. The cytotoxicity of imidacloprid observed in LC-540 cells might be due to its mitochondrial damage and cytoskeletal protein disruption.

1. Introduction

Imidacloprid is a systemic neonicotinoid insecticide widely used to combat agricultural pests and even flea infestation in dogs and cats (Ensley, 2018; Tomizawa and Casida, 2005). The neonicotinoids have a greater affinity for nicotinic acetylcholine receptors (nAChRs) of insects than vertebrates (Tomizawa and Casida, 2005), therefore, it is thought to be less toxic for mammals (Millot et al., 2017). Imidacloprid is registered worldwide as a pesticide to protect various crops (Shao et al., 2013). In 2020, pharmaceutical companies produced approximately 20, 000 tons (Simon-Delso et al., 2015). However, the extensive use of imidacloprid resulted in toxicity in non-target organisms such as bees (Cresswell, 2011), and birds (Hallmann et al., 2014), consequently, its use as seed treatment was prohibited by the European Union in 2013 (European Commission, 2013). The consumption of imidacloprid-treated seed in France has been linked to several mortality events among birds between 1995 and 2014 (Millot et al., 2017). A similar adverse effect of imidacloprid on wild granivorous birds was observed in South Africa's Western Cape province by Botha et al. (2018).

Furthermore, it has been reported that imidacloprid induces male reproductive toxicity (Bal et al., 2012a; Bal et al., 2012b; Hafez et al., 2016; Lonare et al., 2016; Najafi et al., 2010), leading to infertility. Imidacloprid causes a decrease in the number, motility, and viability of sperm in adult Wistar rats (Lonare et al., 2016; Najafi et al., 2010), and albino rats (Hafez et al., 2016). The adverse effects of imidacloprid were attributed to oxidative stress and an increase in polyunsaturated fatty acids caused the decline in Leydig cells, which resulted in a decrease in testosterone levels (Bal et al., 2012a; Bal et al., 2012b).

Leydig cells synthesize testosterone via a complex steroidogenic pathway which is essential for spermatogenesis and reproductive fitness (Andric and Kostic, 2019). Among the complex steps involved in testosterone biosynthesis, is the transport of free cholesterol from the cytoplasm to the mitochondria (Andric and Kostic, 2019), and cytoskeletal proteins might play an essential role in this transfer process (Górowska-Wójtowicz et al., 2018). However, the effects of imidacloprid on the cytoskeletal proteins of Leydig cells remain unclear.

Several authors have proposed that mitochondria are the main target for the toxicity of neonicotinoids, including imidacloprid (Alzahrani, 2019; Cestonaro et al., 2023; Kong et al., 2016; Miao et al., 2022; Xu et al., 2022). Mitochondria are essential in regulating cellular metabolism and are involved in testosterone biosynthesis (Jing et al., 2020). Imidacloprid induced mitochondrial damage by altering mitochondrial calcium homeostasis and inhibiting mitochondrial respiration leading to oxidative stress and cell death (Li et al., 2022; Xu et al., 2022).

* Corresponding author.
E-mail addresses: u17372098@tuks.co.za, wadibrahim352@gmail.com (M. Ibrahim).

https://doi.org/10.1016/j.etap.2023.104310
Received 4 September 2023; Accepted 31 October 2023
Available online 4 November 2023

Therefore, damaged mitochondria can pose a threat to cell survival and influence male fertility (Vakifahmetoglu-Norberg et al., 2017; Xiong et al., 2022).

The objectives of this study were to investigate cell viability and cytotoxicity, evaluate changes in certain cytoskeletal proteins and mitochondria, and assess ultrastructural changes in the rat Leydig tumour cell line (LC-540) exposed to imidacloprid.

2. Materials and methods

2.1. Cell culture and exposure studies

A Fischer rat testis Leydig tumour cell line (LC-540) obtained from the Japanese Collection of Research Bioresources Cell Bank (JCRB9064) was used in this study. Cells were cultured in Eagle's Minimum Essential Medium (EMEM) supplemented with 4 mM L glutamine, 10% fetal bovine serum (FBS), and penicillin-streptomycin (100 U/ml). The cell culture was maintained in an incubator at 37 °C, in a humidified 5% CO_2 environment. The study was approved by the University of Pretoria's Research Ethics Committee (approval number REC030–22).

Additionally, a rat testis was used as a positive control for the immunohistochemical detection of cytokeratin 5, vimentin, and fibronectin and comparison with the labeling in the rat testis Leydig tumour cell line (LC-540).

2.2. Exposure to Imidacloprid

Twenty-four hours prior to exposure, allowing enough time for recovery and stabilization, Leydig cells were seeded in a culture medium supplemented with 5% FBS in tissue culture microplates providing optimum growth area and ease of processing of the cells as required by the different cell assays used in this study. Imidacloprid (No. 37894) was purchased from Sigma-Aldrich, USA; molecular weight of 255.66 g/mol and a purity of 99%. The stock solution of imidacloprid was prepared using 0.03% dimethyl sulfoxide (DMSO) and serially diluted with 5% FBS culture medium to final concentrations for the cytotoxicity studies. The cytotoxic effect of imidacloprid was evaluated in three separate experiments with at least three replicates. To determine the exposure period and imidacloprid concentrations to be used in the additional studies, the results of the MTT assay were interpreted and 72 h was chosen as the incubation period. Concentrations were selected based on the MTT results where declines of around 30% in cell viability occurred (i.e. 300, 400 and 500 μM).

2.3. AlamarBlue® cell viability assay

The viability of Leydig cells exposed to varying concentrations of imidacloprid was evaluated using the alamarBlue® Cell Viability Assay Reagent (1025, Thermo Fisher Scientific). The alamarBlue® cell viability assay is a resazurin-based assay to quantify viable cells in terms of metabolic activity. In the presence of the oxidation-reduction environment in metabolically active cells, resazurin, a non-fluorescent product is reduced to the highly fluorescent resorufin (Bonnier et al., 2015). Following the manufacturer's instructions, the optimum assay conditions, i.e., incubation time, plating density of Leydig cells and fluorescence detector gain setting, were determined. Briefly, cells were seeded in 96 well plates at a density of 500 cells/well and incubated for 24 h before the commencement of the exposure study. Thereafter, the cells were exposed to 200 μL increasing concentrations of imidacloprid (75, 150, 300, 400, 500, 600, 700, and 800 μM) for 24, 48, and 72 h. At the end of the exposure period, the exposure medium was substituted with 100 μL of 10% (v/v) alamarBlue® in the 5% FBS culture medium and incubated for 2 h. Resorufin, the end-product was measured in terms of fluorescence at the following wavelengths: excitation: 530 ± 25 nm and emission: 590 ± 35 nm and fluorescent reader settings: scan points, bottom reading and 35% fluorescence gain, using a Synergy HT BioTek™ multi-mode microplate reader (BIO-TEK Instruments). The cell viability was determined after subtracting the alamarBlue® reduction in the media blank from both the negative control (untreated cells) and treatments and expressed as a percentage of the negative control. A series of dilutions of resorufin in a 5% medium was prepared as a standard for alamarBlue® reduction (not shown).

2.4. MTT cell viability assay

To corroborate the results obtained by the fluorescent alamarBlue® cell viability assay, the colorimetric MTT assay based on the ability of mitochondrial enzymes to reduce the yellow water-soluble tetrazolium salt, 3-[4,5-dimethylthiazole-2-yl]− 2,5-diphenyltetrazolium bromide (MTT) to a purple, insoluble formazan salt (Mosmann, 1983). Cells exposed to a concentration range of imidacloprid as described before were rinsed with 200 μL of phosphate-buffered saline (PBS) (Sigma-Aldrich); before adding 200 μL of incubation medium, followed by 20 μL of MTT (in PBS) (Sigma-Aldrich) and incubated in the dark at 37 °C for 2 h. Thereafter, the medium with MTT was removed and 100 μL of DMSO was added agitating gently for 5 min to dissolve the formazan. The formazan and background absorbances were measured at 570 and 630 nm wavelengths, respectively, using a Synergy HT BioTekTM multi-mode microplate reader (BIO-TEK Instruments). Cell viability was calculated using the formula below:

$$\text{Cell viability}(\%) = \frac{\text{Absorbance of cells treated with Imidacloprid}}{\text{Absorbance of cells with medium only}} \times 100$$

2.5. Immunocytochemistry for Cytokeratin 5, Fibronectin, and Vimentin

Immunocytochemical staining was carried out as previously described by Henn et al. (2022). Briefly, cells were seeded onto an 8-well chamber slide (Lab Tek II, Thermo Scientific) at a concentration of 12 500 cells/400 μL for 24 h, before being exposed to 300, 400, and 500 μM of imidacloprid for 72 h. After exposure, the slides were fixed in 4% formalin for 4 h and transferred to 70% alcohol for at least 10 h. To block the endogenous peroxidase activity, slides were rinsed with a 3% hydrogen peroxide in PBS (pH 7.6) for 5 min. Thereafter, slides were microwaved at 750 W for 21 min in citrate buffer (pH 6) or Tris-EDTA (pH 9). LC-540 cells were incubated with primary antibodies against cytokeratin 5, fibronectin, and vimentin (Table 1). After the slides were washed twice in PBS for 5 min, cells were incubated for 15 min with a horseradish peroxidase (HRP) conjugated secondary antibody (Emergo Europe). To visualize the reactivity, the slides were stained with a 3, 3′-diaminobenzidine solution and then counter-stained with Mayer's hematoxylin. For each slide, at least six images were captured using a digital camera and an Olympus BX-63® light microscope.

To determine the immunolabeling intensity of cytokeratin 5, vimentin, and fibronectin, a semiquantitative analysis was performed using QuPath software (Version 0.3.2) (Bankhead et al., 2017). Based on the optical density around the nucleus, the intensity of the

Table 1
Primary antibodies and immunocytochemical methods.

Antibody (Clone)	Dilution	Incubation time	Antigen Retrieval	Manufacturer
Cytokeratin 5 (polyclonal rabbit, ab53121)	1:50	Overnight	Citrate buffer (pH 6)	Abcam, Cambridge, United Kingdom
Fibronectin (polyclonal rabbit, ab2413)	1:250	1 h	Tris-EDTA (pH 9)	Abcam, Cambridge, United Kingdom
Vimentin (monoclonal mouse 3B4)	1:250	1 h	Citrate buffer (pH 6)	DakoCytomation, Glostrup, Denmark

immunostaining was classified as follows: less than 0.2 (negative), 0.2–0.4 (light), 0.4–0.6 (medium), or more than 0.6 (dark) as described by Henn et al. (2022).

2.6. Fluorescence detection of β-Tubulin and F-actin

Leydig cells were seeded onto 24-well plates at a concentration of 25 000 cells/well for 24 h, before being exposed to 300, 400, and 500 μM imidacloprid for 72 h. In the positive control, cells were incubated with cytochalasin D (Sigma-Aldrich), and vinblastine sulphate (Sigma-Aldrich), for F-actin and ß-Tubulin, respectively. Thereafter, cells were washed once in PBS while being gently agitated for 5 min, followed by 10 min of fixing with 100% ice-cold acetone (Merck) at − 20 °C. Cells were then washed twice in PBS. For F-actin fluorescent labeling, cells were incubated for 30 min at 37 °C in 250 μL of fluorescein isothiocyanate (FITC) labeled phalloidin (Sigma-Aldrich) at a dilution of 1 μg/ml in PBS, while for ß-Tubulin labeling, nonspecific binding sites were blocked with 1% bovine serum albumin (BSA) in PBS at 37 °C for 10 min followed by fluorescent labeling of ß-Tubulin with mouse monoclonal anti-beta tubulin-Cy3 antibody (Sigma-Aldrich), at 37 °C for 1 h at a dilution 1:100 in PBS. The cells were rinsed three times in PBS, with gentle agitation, for 5 min each and then incubated for 15 min at 37 °C with 1.3 μg/ml nuclear counterstain 4′,6-diamidino-2 phenylindole dihydrochloride (DAPI, Sigma-Aldrich). The washing step was then repeated three times. To prevent the sample from drying out, the coverslips were mounted with Prolong Gold Antifade (Invitrogen). Digital images were captured with a Zeiss Confocal microscope LSM-880. Fiji-ImageJ software (Schindelin et al., 2012) with plugins for diffraction PSF 3D and iterative deconvolution 3D (Dougherty, 2005) was used to process the images.

2.7. Evaluation of mitochondrial morphology

Leydig cells were seeded in 24-well plates (25 000 cells/well) and cultured overnight before being exposed to 300, 400, and 500 μM imidacloprid and then cultured for 72 h. After exposure, the incubation medium was removed, and cells were incubated in 500 μL of Mito-Tracker® Orange CMTMRos (Thermo Fisher Scientific) in the dark at 37 °C in a humidified atmosphere with 5% CO_2 for 30 min at a dilution of 0.4 μM/ml in EMEM medium without FBS and Pen-Strep. Thereafter, the cells were washed twice in PBS, with gentle agitation, for 5 min each and then counterstained with DAPI for 15 min at 37 °C. After washing cells twice, cells were fixed with 4% formalin at 37 °C for 10 min and washed twice in PBS for 5 min. Afterwards, cells were post-fixed with 100% ice-cold acetone (Merck) at 20 °C for 10 min and washed two times in PBS. The coverslips were mounted and sealed as described above. Image acquisition was accomplished using a Zeiss Confocal microscope LSM-880 equipped with 100x oil immersion objectives. Based on the method described by Chaudhry et al. (2020), we used the Mitochondria Analyzer plugin of Fiji-ImageJ software (Schindelin et al. (2012), to measure the mitochondrial morphology and network connectivity (branch number, branch length (μm), and branch junctions). The mitochondrial morphology was determined by calculating the mitochondrial size (square area [μm^2]) and perimeter (μm), as well as the mitochondrial shape using the form factor (FF, a measure of mitochondrial length), and aspect ratio (AR, a measure of mitochondrial length and degree of branching) in at least six different microscopic fields per three independent replicates.

2.8. Transmission electron microscopy (TEM)

Leydig cells were cultured in 6-well plates at a concentration of 500 000 cells/well in 5 ml for 24 h, before being exposed to 300, 400, and 500 μM imidacloprid for 72 h. The cells were fixed in 2.5% glutaraldehyde in 0.075 M phosphate buffer (pH 7.4) for at least 15 min. The fixed LC-540 cells were scraped off, transferred to 2 ml Eppendorf tubes, and centrifuged at 1000 x g for 3 min. The cells were then post-fixed in 1% aqueous osmium tetroxide for 1 h, washed with 0.075 M phosphate buffer for 10 min, and dehydrated with serially diluted ethanol solutions (30–100%). The cells were then embedded in TAAB 812 epoxy resin and sectioned using an ultra-microtome (Leica EM UC7). The sections were contrasted with a 2% aqueous solution of uranyl acetate for 10 min and lead citrate for 2 min and images were acquired with a JEOL JEM 1400-FLASH transmission electron microscope (Tokyo, Japan).

2.9. Detection of lysosomal acidity

Changes in the acidic environment of lysosomes in Leydig cells treated with 300, 400, and 500 μM imidacloprid for 72 h, were assessed by using LysoSensor™ Green DND-189 (Invitrogen™, Thermo Fisher Scientific) and following the manufacturer's instructions. After the exposure period, cells were washed twice with PBS and incubated for 30 min at 37 °C in 500 μL of LysoSensor™ Green DND-189) at a dilution of 1 μM/ml in EMEM medium without FBS and penicillin-streptomycin. The cells were rinsed twice in PBS, with gentle agitation, for 5 min each and mounted with Prolong Gold Antifade. Images were acquired using a Zeiss Confocal microscope LSM-880 and analyzed with Fiji-ImageJ software.

2.10. Statistical analysis

AlamarBlue® cell viability and MTT assays were repeated at least three times with three replicates per assay. Cell viability was calculated using Excel. Using IBM SPSS software version 28, a homogeneity of variances test was performed on the data to determine normality, and data were analyzed using Tukey's HSD, post hoc, one-way analysis of variance (ANOVA) to determine the effect of different concentrations, the exposure period by concentration interaction effects, the semi-quantitative analysis for fibronectin and vimentin, the mitochondrial morphology, as well as lysosomal acidity. All significance statements were based on a $P \leq 0.05$.

3. Results

3.1. Effect of imidacloprid on the cell viability

The effect of imidacloprid on the viability of Leydig cells was investigated for 24, 48, and 72 h using the MTT and alamarBlue® viability assays. After 24 h exposure the lowest cell viability of 87.7 ± 6.7% was recorded at 800 μM imidacloprid, when using the alamarBlue® viability assay, with no significant ($P > 0.05$) differences between concentrations of imidacloprid and negative control. However, using the MTT viability assay a significant reduction of 22% in the cell viability (76.0 ± 2.4% cell viability) at 800 μM imidacloprid was calculated.

However, there were dose- and time-dependent effects after 48 and 72 h exposure detected with both MTT and alamarBlue® assays (Fig. 1). There was a significant reduction in viability at the highest concentration of imidacloprid (800 μM), with a decrease of 28% (71.5 ± 3.2% cell viability) and 18% (81.7 ± 1.6% cell viability) for MTT and alamarBlue® assays, respectively, after 48 h exposure, while after 72 h exposure 42% (58.0 ± 0.6% cell viability) and 36% (64.0 ± 4.4% cell viability) for MTT and alamarBlue® assays, respectively (Fig. 1).

3.2. Effect of imidacloprid on the cytokeratin-5, fibronectin, and vimentin structures

Positive immunolabeling for cytokeratin 5, fibronectin, and vimentin was observed as a brown colour in the cytoplasm of Leydig cells as well as in the positive control, i.e., Leydig cells of the rat testis.

In the negative control, cytokeratin 5 immunolabeled the cytoplasm of Leydig cells with homogenous staining throughout the cell. There was

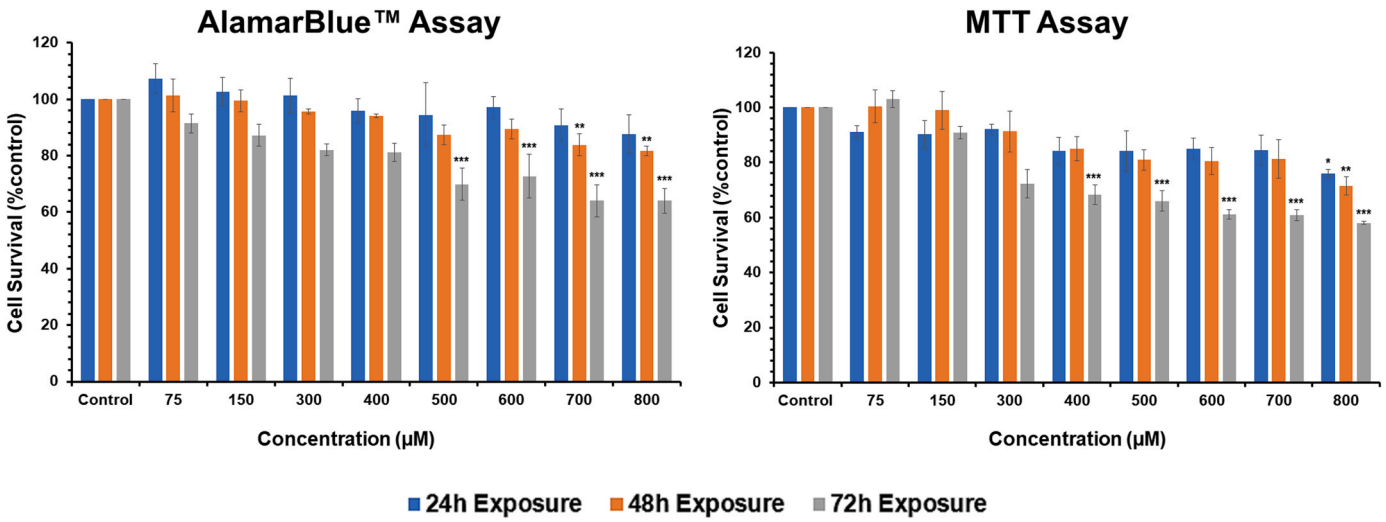

Fig. 1. The effect of imidacloprid exposure on Leydig cell viability after 24, 48, and 72 h.* ,* *,* ** denotes significant differences ($P \leq 0.05$) of the indicated concentrations in relation to control at 24, 48 or 72 h, respectively. Experiments ($n = 3$) were done in triplicate and data are presented as mean ± standard error (SE).

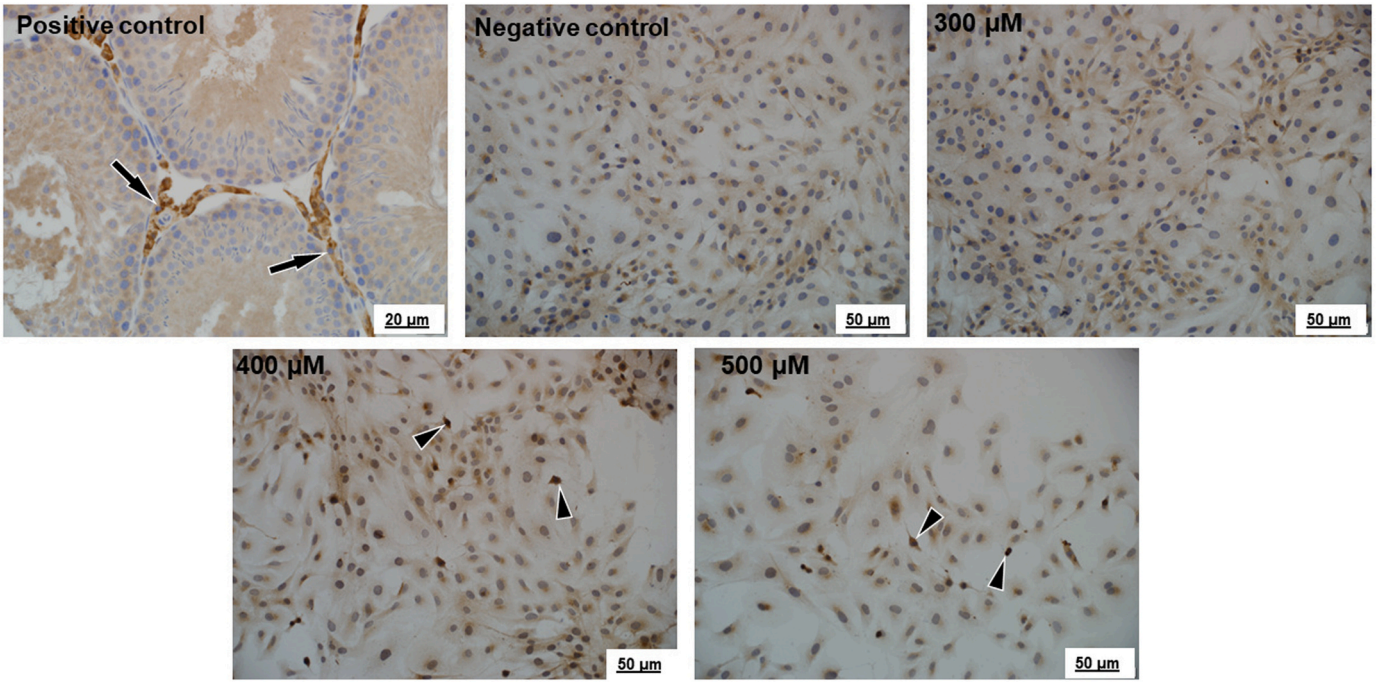

Fig. 2. Immunohistochemical staining of cytokeratin 5 in a rat testis and immunocytochemical labeling of Leydig cells after exposure to 300, 400, and 500 μM imidacloprid for 72 h. Positive control: Arrows indicate immunopositive labeling in the Leydig cells in the testis of the rat. Negative control (media only). Cytokeratin 5 condensations are indicated by arrowheads.

no notable change in the immunolabeling or distribution of cytokeratin 5 following 300 μM imidacloprid exposure of Leydig cells for 72 h. However, at imidacloprid concentrations of 400 and 500 μM, there was a noticeable reduction in the size of affected cells and cytokeratin 5 immunolabeling became more intense or concentrated in their diminished cytoplasm.

In the Leydig cells negative control, fibronectin immunolabeling was observed as dense continuous fibrils throughout the cytoplasm with a dense meshwork of fibrils at the peripheral region. There was no effect on fibronectin fibres in the cells treated with 300 μM imidacloprid compared to the negative control. After exposure to 400 and 500 μM imidacloprid, there was a remarkable loss of fibronectin fibrils, aggregation in the perinuclear region, and loss of its continuous fibrils in the cytoplasm or peripheral cellular region, indicating possible fibronectin failure in cell-cell interaction. Fig. 3.

There were no obvious changes in the immunolabeling and distribution of vimentin intermediate filaments in cells exposed to 300 μM imidacloprid compared to the negative control. However, the number of Leydig cells decreased after exposure to 400 and 500 μM imidacloprid compared to the negative control cells. In addition, there was an aggregation of vimentin immunolabeling in the perinuclear region, which suggests that the intermediate filaments of vimentin were disrupted.

Semiquantitative analysis revealed that fibronectin and vimentin immunostaining intensified around the nuclei of the Leydig cells exposed to 300, 400, and 500 μM of imidacloprid, for 72 h. There was no significant difference in the percentage of vimentin-negative cells

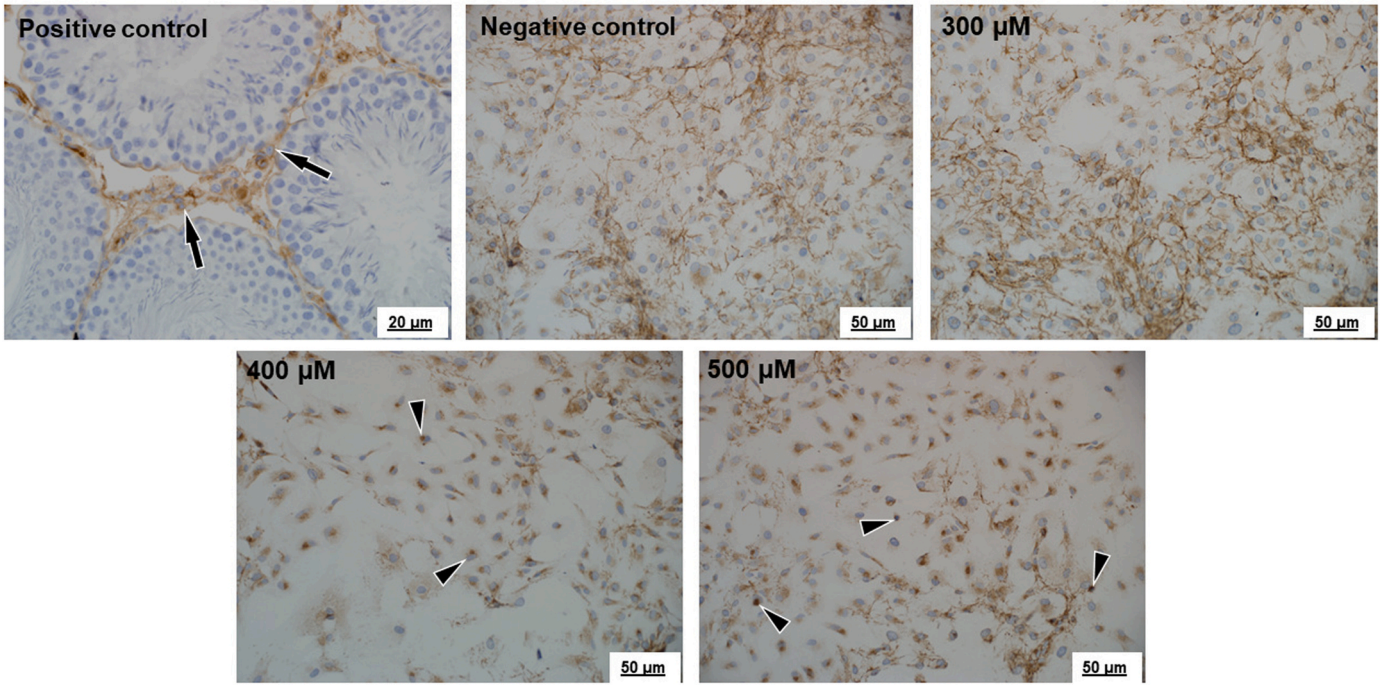

Fig. 3. Immunohistochemical staining of fibronectin in a rat testis and immunocytochemical labeling of Leydig cells after exposure to 300, 400, and 500 µM imidacloprid for 72 h. Positive control: Arrows indicate immunopositive labeling in the Leydig cells in the testis of the rat. Negative control (media only). Perinuclear aggregations of fibronectin are indicated by arrowheads.

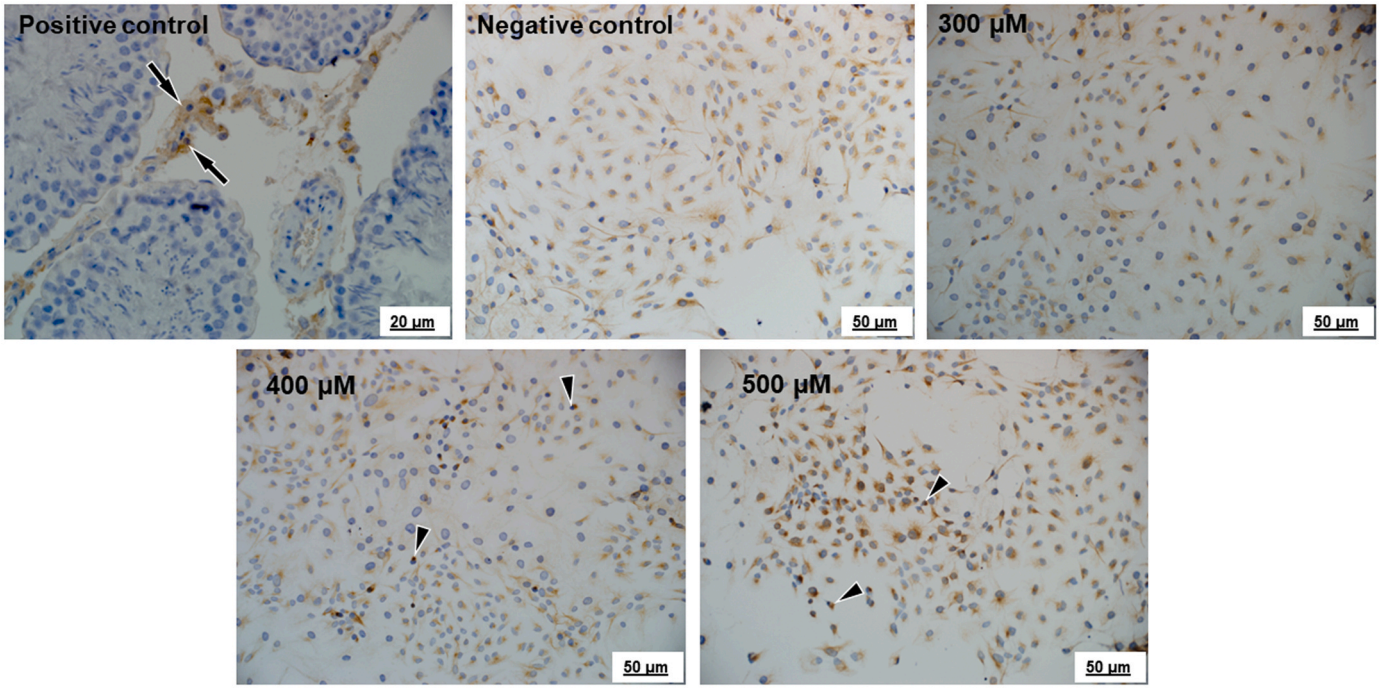

Fig. 4. Immunohistochemical staining of vimentin in a rat testis and immunocytochemical labeling of Leydig cells after exposure to 300, 400, and 500 µM imidacloprid for 72 h. Positive control: Arrows indicate immunopositive labeling in the Leydig cells in the testis of the rat. Negative control (media only). Vimentin aggregates are indicated by arrowheads.

between the treatment and negative control, however, cells treated with 500 µM imidacloprid had a higher percentage of darkly stained vimentin cells. Furthermore, compared to the negative control, cells treated with 300 and 400 µM imidacloprid had a lower percentage of fibronectin-negative cells. However, the percentage of darkly fibronectin-stained cells was higher in cells exposed to 500 µM imidacloprid than in negative control cells. Fig. 5.

3.3. *Effect of imidacloprid on the F-Actin and β-tubulin structures*

Fluorescence labeling of F-actin and β-tubulin in Leydig cells following exposure to 300, 400, and 500 µM imidacloprid for 72 h are

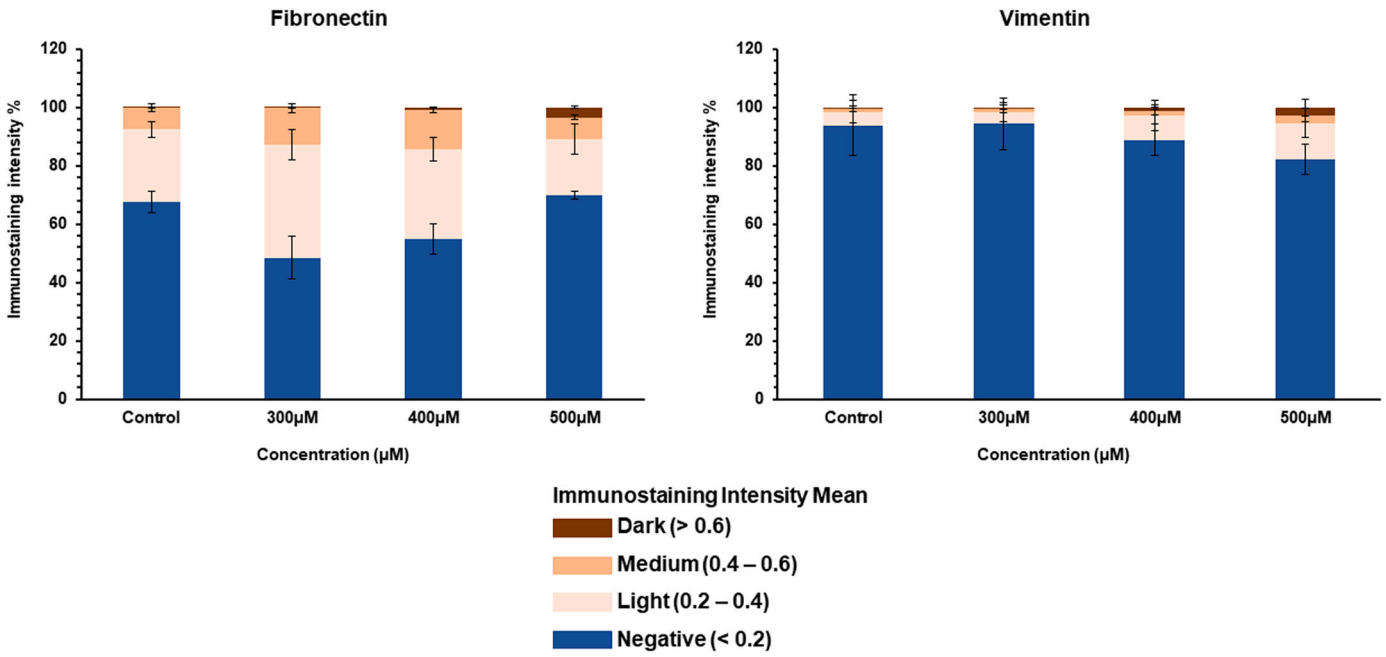

Fig. 5. Semiquantitative analysis of immunostaining intensity of fibronectin and vimentin in Leydig cells following exposure to 300, 400, and 500 μM imidacloprid for 72 h. Data are presented as mean ± standard error (SE).

presented in Figs. 6 and 7. Leydig cells were treated with cytoskeleton-disrupting drugs cytochalasin-D or vinblastine sulphate as positive controls for F-actin and β-tubulin, respectively (Figs. 6 and 7).

In Leydig cells exposed to 300 μM imidacloprid (Fig. 6), no obvious changes were observed in F-actin filaments compared to negative and positive controls, but following exposure to 400 and 500 μM imidacloprid, disorganization of the filament network were observed, including the loss of normal polymerization of F-actin filaments and peripheral aggregation (white arrows). Furthermore, in the cells exposed to 500 μM imidacloprid, the filaments displayed perinuclear aggregation of depolymerized F-actin filaments (red arrows) associated with kidney-shaped nuclei (arrowheads).

Imidacloprid did not induce changes in the structure of the microtubules at concentrations of 300 and 400 μM after 72 h exposure compared to negative and positive controls, while at 500 μM imidacloprid, aggregated and disrupted microtubules were noticed (Fig. 7, arrows).

3.4. *Effect of imidacloprid on the mitochondrial morphology and network*

The Leydig cells stained with a MitoTracker® Orange CMTMRos probe after exposure to 300, 400, and 500 μM imidacloprid for 72 h are presented in Fig. 8A–E. In the control groups, mitochondria appeared to be normally distributed throughout the cytoplasm, while morphological changes were observed in all treatment groups, which became more evident with increasing doses (Fig. 8A-D). Changes included cellular

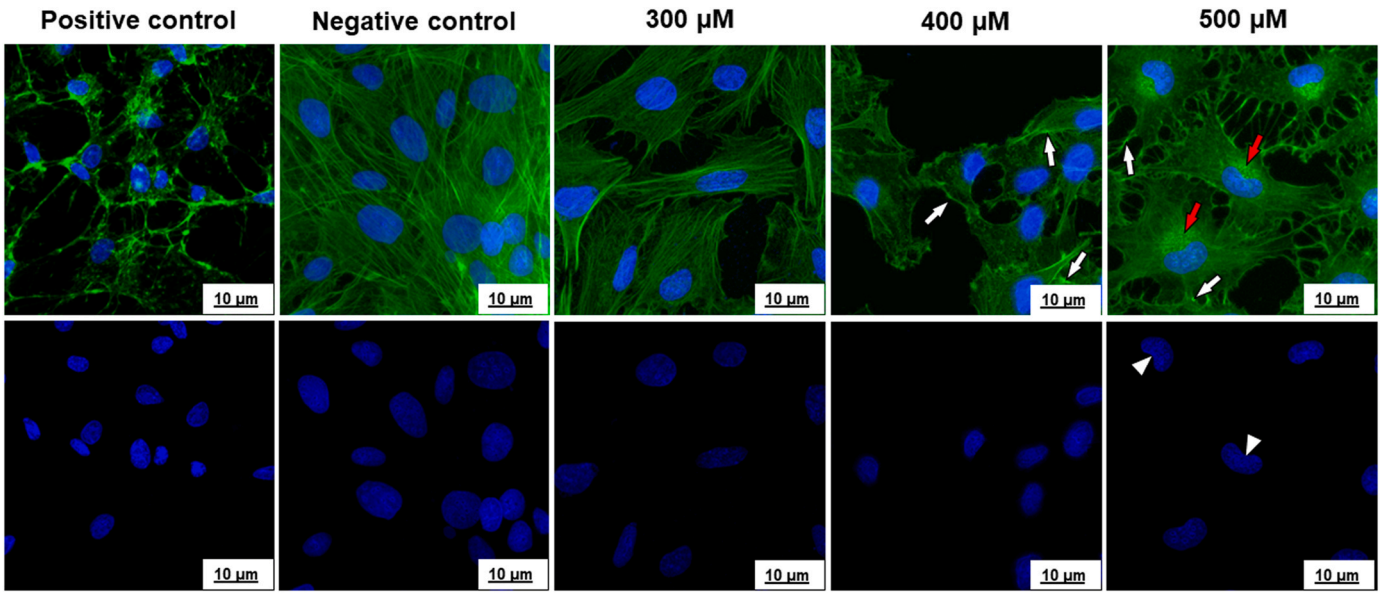

Fig. 6. Fluorescence labeling of F-actin (green) of Leydig cells after exposure to 300, 400, and 500 μM imidacloprid for 72 h. Negative control (media only). Positive control (Cytochalasin-D). White arrows indicate peripheral aggregation of F-actin filaments. Perinuclear aggregation of depolymerized F-actin filaments (red arrows). Kidney-shaped nuclei are counterstained with DAPI (white arrowheads).

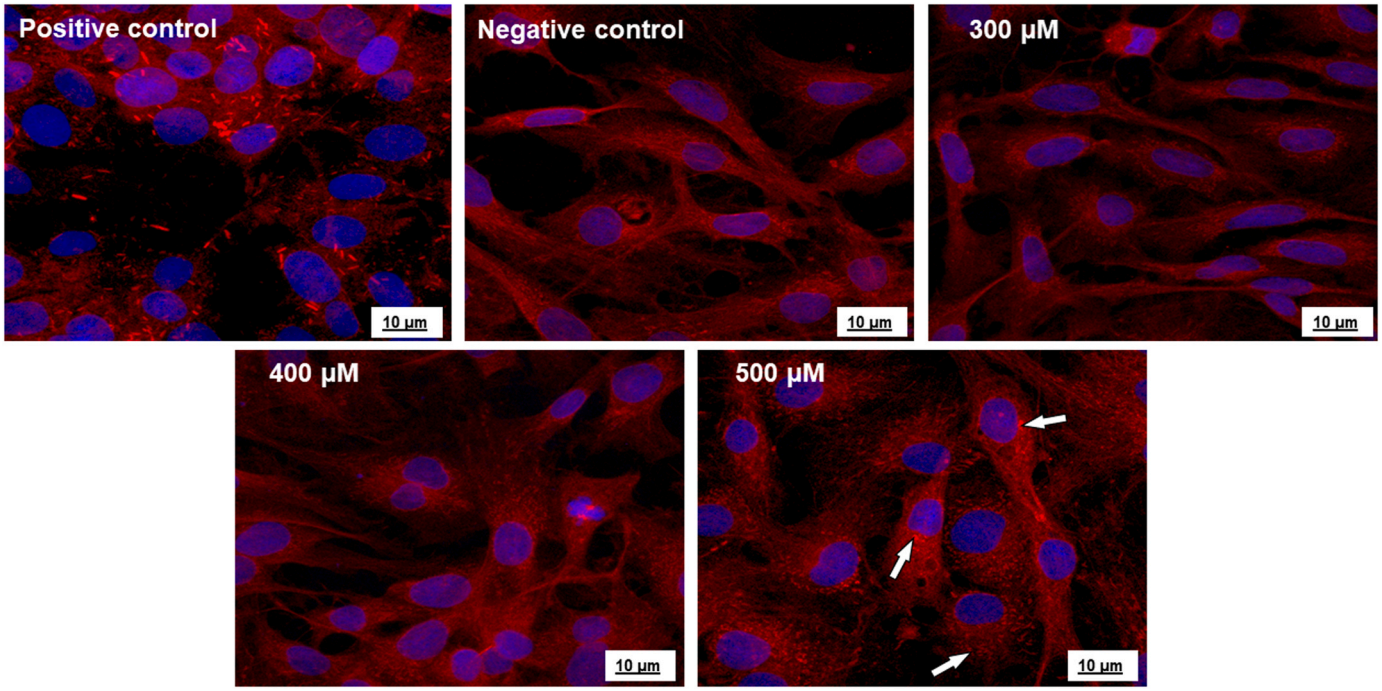

Fig. 7. Fluorescence labeling of β-tubulin (red) of Leydig cells after exposure to 300, 400, and 500 µM imidacloprid for 72 h. Negative control (media only). Positive control (Vinblastine sulphate). Aggregation of disrupted microtubules (arrows). Cell nuclei are counterstained with DAPI (blue).

shrinkage associated with abnormal mitochondrial distribution. Furthermore, the quantitative analysis of the mitochondrial morphology revealed a significant decrease in the size (area and perimeter) and length (form factor and aspect ratio) of mitochondria of the cells in all treatment groups compared to controls (Fig. 8E). The mitochondrial network parameters including the branch number, branch lengths, and branch junctions were significantly reduced in all treated groups compared to control (Fig. 8F), indicating possible mitochondrial fragmentation in treated cells.

3.5. Ultrastructure and lysosomal acidity

The ultrastructural changes in Leydig cells after exposure to 300, 400, and 500 µM imidacloprid for 72 h are presented in Fig. 9A. Damaged mitochondria and cytoplasmic vacuoles were observed in all treated groups in comparison to the control group (Fig. 9A). The damaged mitochondria were characterized by swelling, loss of cristae and rupture of outer membranes. Furthermore, lysosomes and distinct autophagic vacuoles containing damaged mitochondria and other cellular organelles were also observed in cells exposed to 400 and 500 µM imidacloprid (Fig. 9A).

It is well known that autophagy delivers cytoplasmic material and damaged organelles to lysosomes for degradation. Thus, we stained living cells with LysoSensor™ Green DND-189 to quantify the lysosomal acidity, which revealed that imidacloprid significantly increased lysosomal acidity in all treatments compared with the control (Fig. 9B and C).

4. Discussion

In recent years, global concerns grew regarding the decline of male reproductive capability (Tong et al., 2022). Studies have confirmed that exposure to environmental toxicants might be one of the primary reasons (Mann et al., 2020; Mendy and Pinney, 2022). Imidacloprid, a neonicotinoid insecticide, is highly soluble in water, therefore it can easily accumulate in ground and surface water causing adverse environmental effects (Demirak, 2019; Hrybova et al., 2019; Tišler et al., 2009). It has been reported that exposure to imidacloprid affects male fertility in rabbits and rats (Alamgir Kobir et al., 2023; Saber et al., 2021). Leydig cells are responsible for testosterone synthesis to maintain spermatogenesis and reproductive fitness and are susceptible to environmental toxicants (Chen et al., 2010; Zhang et al., 2022b), including imidacloprid (Bal et al., 2012b; Zhao et al., 2021). In the current study, imidacloprid had a cytotoxic effect on Leydig cells in vitro (Fig. 1). To our knowledge, there have been no studies reporting the cytotoxic effects of imidacloprid on the Leydig cell line; but it has been reported that imidacloprid caused cytotoxicity in a human hepatoblastoma (HepG2) cell line (Conte et al., 2022; Guimarães et al., 2022), human prostate epithelial (WPM-Y.1) cell line (Abdel-Halim and Osman, 2020), and Chinese hamster ovary (CHO-K1) cell line (Al-Sarar et al., 2015). Among these, Conte et al. (2022) reported that exposure to a commercial formulation of imidacloprid (60% purity) at 663.66 mg/L (2654.64 µM) induced a 50% effect in HepG2 cells after 48 h. Other authors also indicated that exposure to the pure form of 500–2000 µM imidacloprid for 24 and 48 h induced a significant decrease in HepG2 cell viability (Guimarães et al., 2022). In the present study, a notable reduction in the viability of cells treated with imidacloprid concentrations of 800 µM for 48 h or above 300 µM for 72 h, based on the MTT assay, was observed, and was also confirmed with the alamarBlue® assay. The MTT assay evaluates the mitochondrial activity, while the alamarBlue® assay measures the total cell viability, thus verifying that Leydig cells are indeed susceptible to toxicity induced by imidacloprid.

Cytoskeletal proteins, including microtubules, intermediate filaments, and microfilaments, are interconnected filamentous structures that extend throughout the cytoplasm of the cell and even the extracellular matrix. These proteins play a crucial role in cellular processes such as intercellular and intracellular communication, maintenance of cellular morphology and cell division (Jimenez-Lopez, 2017). Additionally, intermediate filaments, microtubules, and microfilaments are essential in the regulation of hormone biosynthesis in the gonads (Stocco and Clark, 1996; Wu and Zhang, 2022), and it is thus reasonable to deduce that depolymerization of these proteins might have a negative impact on testicular function.

The intermediate filament, cytokeratin 5 is a type II cytokeratin,

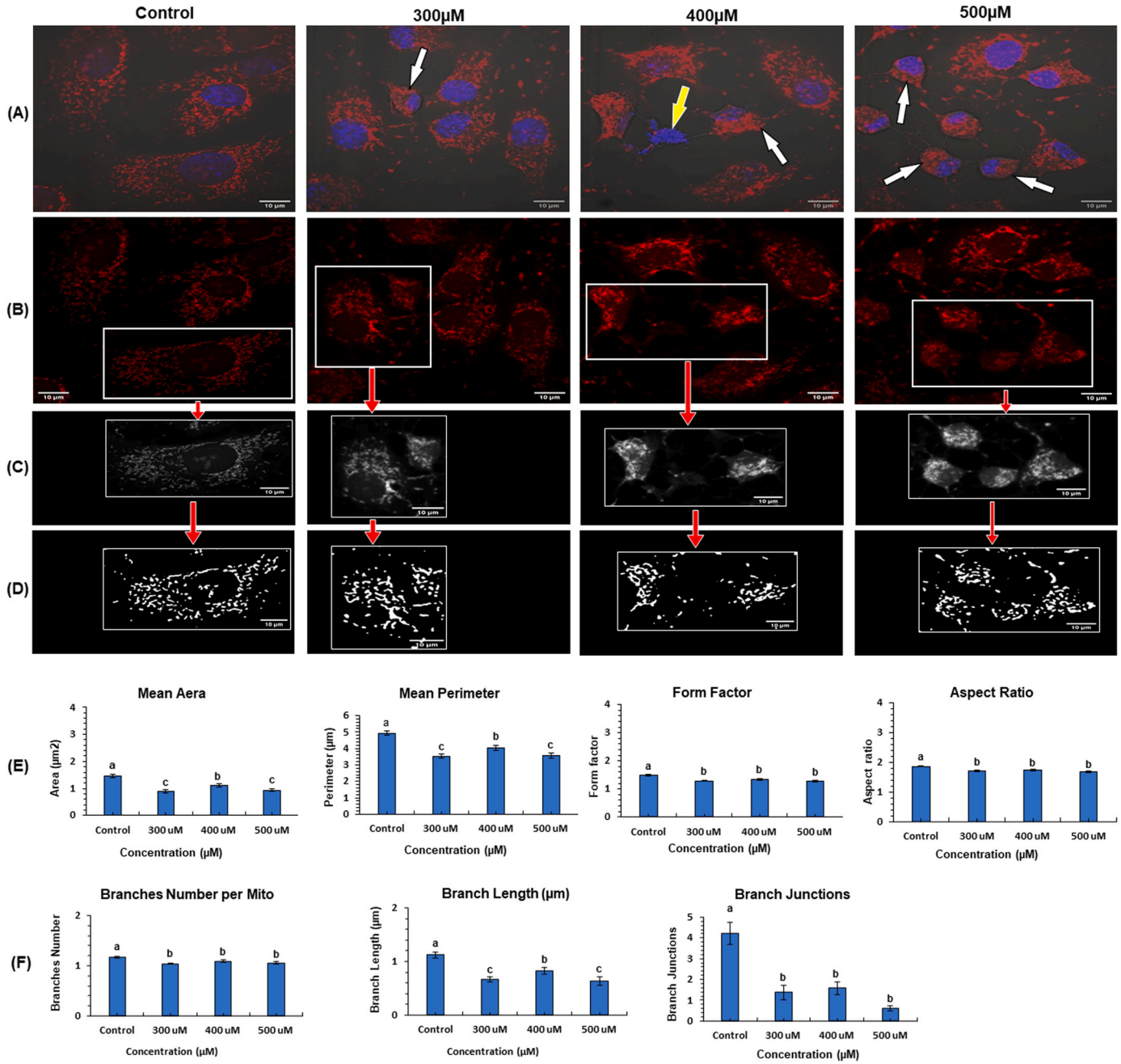

Fig. 8. Effect of 72 h exposure to 300, 400, and 500 μM imidacloprid on the mitochondrial morphology and network in Leydig cells. (A) Mitochondria were stained with Mitotracker Orange (red), while the nuclei were counterstained with DAPI (blue). White arrows indicate abnormal distribution of fragmented mitochondria in the cytoplasm of treated cells. The yellow arrow indicates damaged nuclei. (B & C) ROI-1 (Region of Interest) shows the sum of the z-stack cell before optimization with the plugin - Mitochondrial Analyzer of the Fiji-ImageJ software. (D) ROI-2 shows the threshold result of cells after optimization. A quantitative analysis of (E) morphological, and (F) network connectivity of mitochondria in all treatment and control groups ($n = 3$ replicates). Data are presented as mean ± standard error (SE). ^{a,b,c} Indicates differences between groups with $P \leq 0.05$.

which plays a crucial role in modulating the proliferation and differentiation of the cells in stratified epithelia (Alam et al., 2011). In the current study, LC-540 cells exposed to imidacloprid exhibited condensation of cytokeratin 5 intermediate filaments, and the affected cells were smaller in size. In addition to the expression of cytokeratin 5 in basal cells of the stratified epithelium lining the skin and digestive tract (Ramírez et al., 1994), it is also expressed in the epithelial cells of the male reproductive tract of humans (Achtstätter et al., 1985), vampire bats (Castro et al., 2017), and Japanese quails (Ibrahim et al., 2022). Positive cytokeratin 5 immunolabeling was also detected in Leydig cells of rat testis used as a positive control (Fig. 2). Therefore, considering the expression of cytokeratin 5 in Leydig cells and its disruption by imidacloprid in this study, further investigations are needed to study the possible function of cytokeratin 5 in the male reproductive organs, particularly in Leydig cells.

Imidacloprid induced a decrease in fibronectin fibrils, perinuclear aggregation, and loss of cytoplasmic and peripheral-continuous fibronectin networks in the current study. A study on zebrafish testis indicated that imidacloprid induces hypertrophy in Leydig cells and interstitial testicular fibrosis (Akbulut, 2021). The polymerization of fibronectin fibrils is essential to cell survival, proliferation, adhesion, and migration (Mosher and Furcht, 1981). Additionally, fibronectin

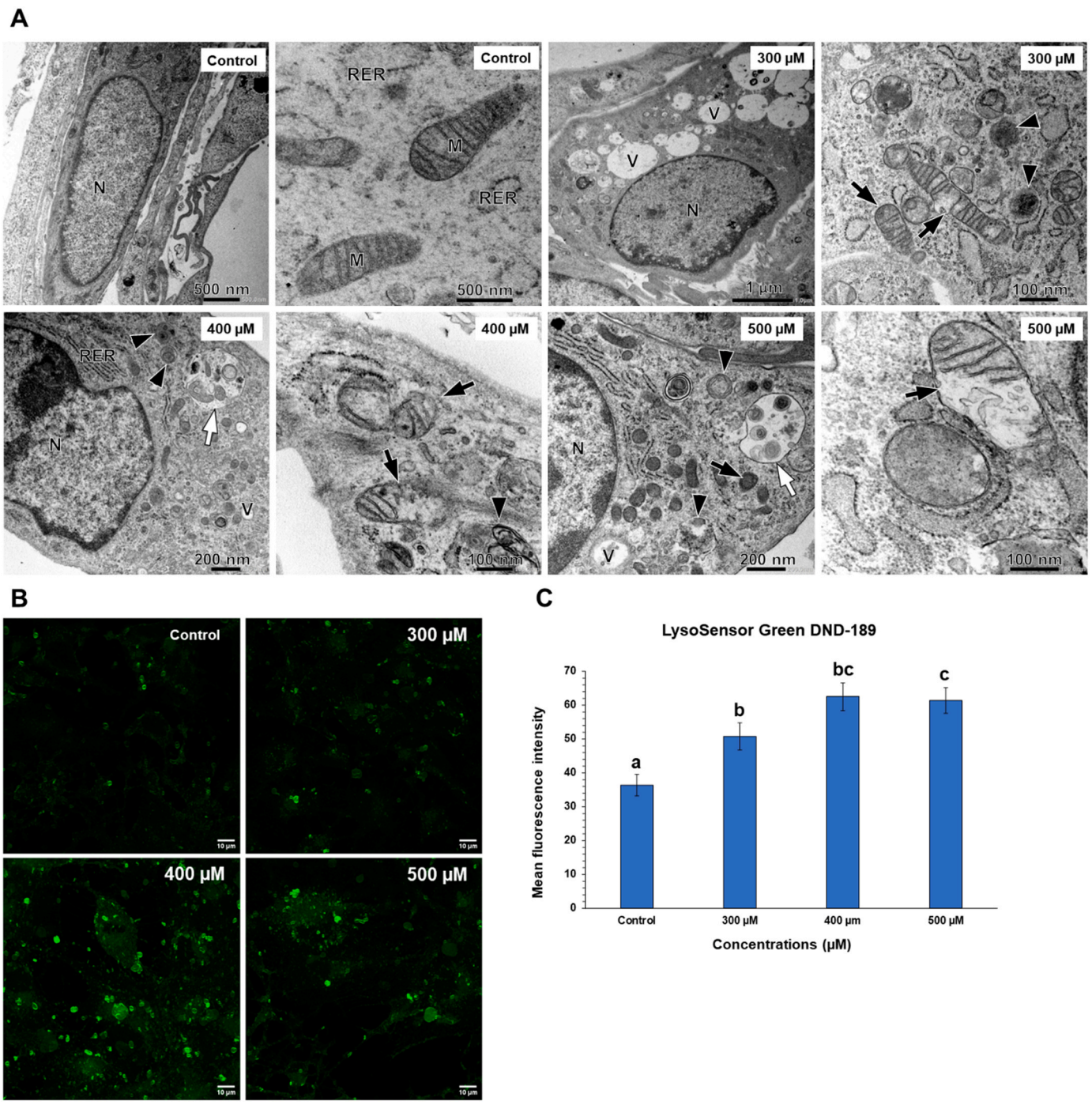

Fig. 9. (A) Transmission electron micrographs of Leydig cells exposed to 300, 400, and 500 µM imidacloprid for 72 h. Damaged mitochondria (black arrows) and lysosomes (black arrowheads). White arrows indicate distinct autophagic vacuoles with mitochondria and cellular debris. M, Mitochondria; N, Nucleus; RER, Rough Endoplasmic Reticulum; V, Vacuole. (B) Lysosomal acidity detection by LysoSensor™ Green DND-189. (C) Quantification of the fluorescence intensity of lysosomal acidity. All data are representative of three independent experiments and presented as mean ± (S.E). ^{a,b,c} Indicates differences between groups with $P \leq 0.05$.

contributes to inflammatory reactions and the deposition of extracellular matrix during the development of fibrotic diseases (Tiwari et al., 2016). Diaz et al. (2002) suggested that the fibronectin extracellular matrix modulates steroidogenic processes in Leydig cells in vitro. Therefore, imidacloprid exposure might induce male infertility by disrupting the polymerization of fibronectin fibrils in the Leydig cell.

In the present study, there was a disruption and disorganization of F-actin microfilaments, vimentin intermediate filaments and microtubules in Leydig cells following exposure to 400 and 500 µM imidacloprid for 72 h (Figs. 4, 6 and 7). F-actin microfilaments became depolymerized with peripheral and perinuclear aggregation of the filaments while β-tubulin-labeling of microtubules demonstrated aggregation and disruption in cells treated with 500 µM imidacloprid. Additionally, there were perinuclear aggregation and disorganization of the vimentin intermediate filaments in cells exposed to 400 and 500 µM imidacloprid. Cytoskeletal proteins such as actin, tubulin, and vimentin are expressed in the Leydig cells (Bilińska, 1993). Besides their numerous functions in general cellular processes, these proteins are also involved in Leydig cell steroidogenic processes (Sewer and Li, 2008). Studies have demonstrated that these proteins are involved in the transportation of

cholesterol from lipid droplets into mitochondria (Clark and Shay, 1981; Hall and Almahbobi, 1997; Li et al., 2016), and their role in the steroidogenic process was confirmed (Wu and Zhang, 2022). The disorganization and disruption in the F-actin microfilaments, microtubules, and vimentin intermediate filaments observed in this study might explain the decrease in testosterone levels in adult male rats, which were experimentally treated with imidacloprid (Bal et al., 2012a; Bal et al., 2012b), thus suggesting that imidacloprid might decrease the testosterone levels through cytoskeletal disruption.

Mitochondria are essential in cellular metabolism, and the response to stresses (Vakifahmetoglu-Norberg et al., 2017), and they play a major role in testosterone biosynthesis (Zirkin and Papadopoulos, 2018). Therefore, any changes in the mitochondrial structure are closely linked to male infertility. In this study, we observed that imidacloprid altered the mitochondrial morphology in all treated cells. Changes included swelling, loss of cristae, and rupture of outer membranes (Fig. 9A). Similarly, damaged and swollen mitochondria were reported in a gill cell line of flounder exposed to 60 μg/ml (240 μM) imidacloprid for 48 h (Su et al., 2007). Recently, an increase in mitochondrial depolarization has been reported in human colorectal adenocarcinoma cells (HT-29) treated with pure and commercial formulations of 800, 1600, and 3200 μM imidacloprid (Baysal and Atlı-Eklioğlu, 2021), and in macrophage (RAW 264.7) cells exposed to a commercial formulation of 150, 500, and 1000 mg/L (600, 2000 and 4000 μM) imidacloprid for 24 and 96 h (Cestonaro et al., 2023), indicating that mitochondria are the main target of imidacloprid cytotoxicity (Cestonaro et al., 2023). In addition, we used a Mitotracker Orange probe to detect the mitochondrial morphology and network. Imidacloprid exposure exhibited a significant decrease in mitochondrial size, length, as well as network connectivity in all treatment groups (Fig. 8A–F). Degeneration, swelling and loss of cristae in the spermatozoal mitochondria of the red palm weevil, a snout beetle (Alzahrani, 2019) and in the Kenyon cells in the mushroom bodies of the honeybee brain (Catae et al., 2018) were also observed after treatments with imidacloprid.

Furthermore, there were autophagic vacuoles and lysosomes in cells treated with 400 and 500 μM imidacloprid (Fig. 9A). Imidacloprid exposure induces autophagy in the kidney cell line (CIK cell) of the grass carp (Li et al., 2022), and the midgut epithelial cells of honeybees (Carneiro et al., 2022). Autophagy is an essential cellular process that amongst others selectively removes damaged and defective mitochondria, which are ultimately conveyed to the lysosomes for bulk degradation (Maiuri et al., 2007; Morales et al., 2020), thus protecting cells from the metabolic stresses of damaged mitochondria (Zhang et al., 2022a). Lysosomal content is acidic and digests the autophagic material, including damaged mitochondria (Xu and Ren, 2015). In this study, we further analyzed whether imidacloprid increased the lysosomal acidity in the Leydig cells by using LysoSensor™ Green DND-189. We found that imidacloprid induced a significant increase in lysosomal acidity in all treated cells compared with the control (Fig. 9B&C). The autophagic vacuoles and the lysosomal acidity in Leydig cells in the present study indicate cellular responses to imidacloprid toxicity. As this study examined the cytotoxicity of imidacloprid in its pure form, future studies are needed to compare an in vitro and in vivo effects of commercial formulations of this compound on Leydig cells.

5. Conclusion

In conclusion, imidacloprid exposure decreased a rat Leydig (LC-540) cell line's viability in vitro in a time- and dose-dependent manner. Imidacloprid induced a disruption and disorganization of cytokeratin 5, fibronectin, F-actin, vimentin, and β-tubulin proteins, as well as mitochondrial damage in the LC-540 cells. The results of this study suggest that the reduction in the viability of LC-540 cells could be due to the changes in mitochondrial morphology and cytoskeletal protein disruption induced by imidacloprid. Seeing that mitochondria and cytoskeletal proteins in Leydig cells play a crucial role in steroidogenic activity, it is possible to speculate that imidacloprid might cause male infertility.

Declaration of Competing Interest

The authors declare that they have no known competing financial interests or personal relationships that could have appeared to influence the work reported in this paper.

Acknowledgements

The technical assistance of Rephima Phaswane and Naomi Timmerman (Pathology Section, Department of Paraclinical Sciences) and Dr Antoinette Lensink (Electron Microscope Unit, Onderstepoort campus) in this study is greatly acknowledged. Mohammed Ibrahim would like to thank the University of Pretoria for financial support through a Co-funded Post-Doctoral Fellowship.

References

Abdel-Halim, K.Y., Osman, S.R., 2020. Cytotoxicity and oxidative stress responses of imidacloprid and glyphosate in human prostate epithelial WPM-Y. 1 cell line. J. Toxicol. 2020 https://doi.org/10.1155/2020/4364650.

Achtstätter, T., Moll, R., Moore, B., Franke, W.W., 1985. Cytokeratin polypeptide patterns of different epithelia of the human male urogenital tract: immunofluorescence and gel electrophoretic studies. J. Histochem. Cytochem. 33, 415–426. https://doi.org/10.1177/33.5.2580881.

Akbulut, C., 2021. Acute exposure to the neonicotinoid insecticide Imidacloprid of Zebrafish (*Danio rerio*) Gonads: a histopathological approach. Ann. Limnol. Int. J. Lim. 57, 23. https://doi.org/10.1051/limn/2021021.

Alam, H., Sehgal, L., Kundu, S.T., Dalal, S.N., Vaidya, M.M., 2011. Novel function of keratins 5 and 14 in proliferation and differentiation of stratified epithelial cells. Mol. Biol. Cell. 22, 4068–4078. https://doi.org/10.1091/mbc.e10-08-0703.

Alamgir Kobir, M., Akter, L., Sultana, N., Pervin, M., Abdul Awal, M., Rabiul Karim, M., 2023. Effects of imidacloprid-contaminated feed exposure on spermatogenic cells and Leydig cells in testes of adult male rabbits (*Oryctolagus cuniculus*). Saudi J. Biol. Sci. 30, 103541 https://doi.org/10.1016/j.sjbs.2022.103541.

Al-Sarar, A.S., Abobakr, Y., Bayoumi, A.E., Hussein, H.I., 2015. Cytotoxic and genotoxic effects of abamectin, chlorfenapyr, and imidacloprid on CHOK1 cells. Environ. Sci. Pollut. Res. 22, 17041–17052. https://doi.org/10.1007/s11356-015-4927-3.

Alzahrani, A.M., 2019. Ultrastructural damage and biochemical alterations in the testes of red palm weevils (Rhynchophorus ferrugineus) exposed to imidacloprid. Environ. Sci. Pollut. Res. 26, 16548–16555. https://doi.org/10.1007/s11356-019-04968-8.

Andric, S.A., Kostic, T.S., 2019. Regulation of Leydig cell steroidogenesis: intriguing network of signaling pathways and mitochondrial signalosome. Curr. Opin. Endocr. Metab. Res. 6, 7–20. https://doi.org/10.1016/j.coemr.2019.03.001.

Bal, R., Naziroğlu, M., Türk, G., Yilmaz, Ö., Kuloğlu, T., Etem, E., Baydas, G., 2012a. Insecticide imidacloprid induces morphological and DNA damage through oxidative toxicity on the reproductive organs of developing male rats. Cell Biochem. Funct. 30, 492–499. https://doi.org/10.1002/cbf.2826.

Bal, R., Türk, G., Tuzcu, M., Yilmaz, O., Kuloglu, T., Gundogdu, R., Gür, S., Agca, A., Ulas, M., Çambay, Z., 2012b. Assessment of imidacloprid toxicity on reproductive organ system of adult male rats. J. Environ. Sci. Health B 47, 434–444. https://doi.org/10.1080/03601234.2012.663311.

Bankhead, P., Loughrey, M.B., Fernández, J.A., Dombrowski, Y., Mcart, D.G., Dunne, P. D., Mcquaid, S., Gray, R.T., Murray, L.J., Coleman, H.G., 2017. QuPath: open source software for digital pathology image analysis, V0.3.2 (Version 0.3.2). Sci. Rep. 7, 1–7. https://doi.org/10.1038/s41598-017-17204-5.

Baysal, M., Atlı-Eklioğlu, Ö., 2021. Comparison of the toxicity of pure compounds and commercial formulations of imidacloprid and acetamiprid on HT-29 cells: Single and mixture exposure. Food Chem. Toxicol. 155, 112430 https://doi.org/10.1016/j.fct.2021.112430.

Bilińska, B., 1993. Coexistence of tubulin, vimentin and F-actin in Leydig cells in vitro detected by double immunofluorescence studies. Cytobios 74, 15–21.

Bonnier, F., Keating, M., Wrobel, T.P., Majzner, K., Baranska, M., Garcia-Munoz, A., Blanco, A., Byrne, H.J., 2015. Cell viability assessment using the Alamar blue assay: a comparison of 2D and 3D cell culture models. Toxicol. Vitr. 29, 124–131. https://doi.org/10.1016/j.tiv.2014.09.014.

Botha, C.J., Du Plessis, E.C., Coetser, H., Rosemann, M., 2018. Analytical confirmation of imidacloprid poisoning in granivorous Cape spurfowl (Pternistis capensis). J. S. Afr. Vet. Assoc. 89, 1–5. ⟨https://hdl.handle.net/10520/EJC-f98b9fc59⟩.

Carneiro, L.S., Martinez, L.C., De Oliveira, A.H., Cossolin, J.F.S., De Resende, M.T.C.S., Gonçalves, W.G., Medeiros-Santana, L., Serrão, J.E., 2022. Acute oral exposure to imidacloprid induces apoptosis and autophagy in the midgut of honey bee Apis mellifera workers. Sci. Total Environ. 815, 152847 https://doi.org/10.1016/j.scitotenv.2021.152847.

Castro, M.M., Kim, B., Hill, E., Fialho, M.C., Puga, L.C., Freitas, M.B., Breton, S., Machado-Neves, M., 2017. The expression patterns of aquaporin 9, vacuolar H+-ATPase, and cytokeratin 5 in the epididymis of the common vampire bat. Histochem. Cell Biol. 147, 39–48. https://doi.org/10.1007/s00418-016-1477-9.

Catae, A.F., Roat, T.C., Pratavieira, M., Silva Menegasso, A.R.D., Palma, M.S., Malaspina, O., 2018. Exposure to a sublethal concentration of imidacloprid and the side effects on target and nontarget organs of Apis mellifera (Hymenoptera, Apidae). Ecotoxicology 27, 109–121. https://doi.org/10.1007/s10646-017-1874-4.

Cestonaro, L.V., Crestani, R.P., Conte, F.M., Piton, Y.V., Schmitz, F., Ferreira, F.S., Wyse, A.T.S., Garcia, S.C., Arbo, M.D., 2023. Immunomodulatory effect of imidacloprid on macrophage RAW 264.7 cells. Environ. Toxicol. Pharmacol. 101, 104190 https://doi.org/10.1016/j.etap.2023.104190.

Chaudhry, A., Shi, R., Luciani, D.S., 2020. A pipeline for multidimensional confocal analysis of mitochondrial morphology, function, and dynamics in pancreatic β-cells. Am. J. Physiol. Endocrinol. Metab. 318, E87–E101. https://doi.org/10.1152/ajpendo.00457.2019.

Chen, H., Zhou, L., Lin, C.-Y., Beattie, M.C., Liu, J., Zirkin, B.R., 2010. Effect of glutathione redox state on Leydig cell susceptibility to acute oxidative stress. Mol. Cell. Endocrinol. 323, 147–154. https://doi.org/10.1016/j.mce.2010.02.034.

Clark, M.A., Shay, J.W., 1981. The role of tubulin in the steroidogenic response of murine adrenal and rat Leydig cells. Endocrinology 109, 2261–2263. https://doi.org/10.1210/endo-109-6-2261.

Conte, F.M., Cestonaro, L.V., Piton, Y.V., Guimarães, N., Garcia, S.C., Dias Da Silva, D., Arbo, M.D., 2022. Toxicity of pesticides widely applied on soybean cultivation: synergistic effects of fipronil, glyphosate and imidacloprid in HepG2 cells. Toxicol. Vitr. 84, 105446 https://doi.org/10.1016/j.tiv.2022.105446.

Cresswell, J.E., 2011. A meta-analysis of experiments testing the effects of a neonicotinoid insecticide (imidacloprid) on honey bees. Ecotoxicology 20, 149–157. https://doi.org/10.1007/s10646-010-0566-0.

Demirak, M.Ş.Ş., 2019. Determination of insecticide imidacloprid residues in Tokat city water by using enzyme-linked immunosorbant assay (ELISA). J. BAUN Inst. Sci. Technol. 21, 708–715. https://doi.org/10.25092/baunfbed.637064.

Dougherty, R., 2005. Extensions of DAMAS and benefits and limitations of deconvolution in beamforming, 11th AIAA/CEAS aeroacoustics conference, Monterey, California, 2961. ⟨https://doi.org/10.2514/6.2005–2961⟩.

Ensley, S.M., 2018. Neonicotinoids. In: Gupta, R.C. (Ed.), Veterinary Toxicology: Basic and Clinical Principles. Academic Press, pp. 521–524. https://doi.org/10.1016/B978-0-12-811410-0.00040-4.

European Commission, 2013. Commission Implementing Regulation (EU), No 485/2013 of 24 May 2013, amending Implementing Regulation (EU) No 540/2011, as regards the conditions of approval of the active substances clothianidin, thiamethoxam and imidacloprid, and prohibiting the use and sale of seeds treated with plant protection products containing those active substances. O. J. E. U. 139, 12–26.

Górowska-Wójtowicz, E., Dutka, P., Kudrycka, M., Pawlicki, P., Milon, A., Plachno, B., Tworzydlo, W., Pardyak, L., Kaminska, A., Hejmej, A., 2018. Regulation of steroidogenic function of mouse Leydig cells: G-coupled membrane estrogen receptor and peroxisome proliferator-activated receptor partnership. J. Physiol. Pharm. 69 https://doi.org/10.26402/jpp.2018.3.04.

Guimarães, A.R.D.J.S., Bizerra, P.F.V., Miranda, C.A., Mingatto, F.E., 2022. Effects of imidacloprid on viability and increase of reactive oxygen and nitrogen species in HepG2 cell line. Toxicol. Mech. Methods 32, 204–212. https://doi.org/10.1080/15376516.2021.1992553.

Hafez, E.M., Issa, S.Y., Al-Mazroua, M.K., Ibrahim, K.T., Rahman, S.M.A., 2016. The neonicotinoid insecticide imidacloprid: a male reproductive system toxicity inducer-human and experimental study, 2476-2067.1000109 Toxicol. Open Access 2. https://doi.org/10.4172/2476-2067.1000109.

Hall, P.F., Almahbobi, G., 1997. Roles of microfilaments and intermediate filaments in adrenal steroidogenesis. Microsc. Res. Tech. 36, 463–479. https://doi.org/10.1002/(SICI)1097-0029(19970315)36:6%3C463::AID-JEMT4%3E3.0.CO;2-J.

Hallmann, C.A., Foppen, R.P., Van Turnhout, C.A., De Kroon, H., Jongejans, E., 2014. Declines in insectivorous birds are associated with high neonicotinoid concentrations. Nature 511, 341–343. https://doi.org/10.1038/nature13531.

Henn, D., Venter, A., Ferreira, G.C., Botha, C.J., 2022. The in vitro cytotoxic effects of ionophore exposure on selected cytoskeletal proteins of C2C12 myoblasts. Toxins 14, 447. https://doi.org/10.3390/toxins14070447.

Hrybova, N.Y., Khyzhan, O., Maksin, V., Kavshun, L., Tankha, O., 2019. Determination of xenobiotic imidacloprid content in surface waters. J. Water Chem. Technol. 41, 313–317. https://doi.org/10.3103/S1063455×19050072.

Ibrahim, M.I., Williams, J.H., Botha, C.J., 2022. Immunohistochemical changes in the testicular excurrent duct system of healthy, Male Japanese Quail (*Coturnix coturnix japonica*) Observed at 4, 6–7, 12, and 52 weeks of age. Int. J. Mol. Sci. 23, 14028. https://doi.org/10.3390/ijms232214028.

Jimenez-Lopez, J.C., 2017. Cytoskeleton: Structure, Dynamics, Function and Disease. InTech, Rijeka, Croatia. https://doi.org/10.5772/62622.

Jing, J., Ding, N., Wang, D., Ge, X., Ma, J., Ma, R., Huang, X., Jueraitetibaike, K., Liang, K., Wang, S., Cao, S., Zhao, A.Z., Yao, B., 2020. Oxidized-LDL inhibits testosterone biosynthesis by affecting mitochondrial function and the p38 MAPK/COX-2 signaling pathway in Leydig cells. Cell Death Dis. 11, 626. https://doi.org/10.1038/s41419-020-02751-z.

Kong, D., Zhang, J., Hou, X., Zhang, S., Tan, J., Chen, Y., Yang, W., Zeng, J., Han, Y., Liu, X., Xu, D., Cai, R., 2016. Acetamiprid inhibits testosterone synthesis by affecting the mitochondrial function and cytoplasmic adenosine triphosphate production in rat Leydig cells. Biol. Reprod. 96, 254–265. https://doi.org/10.1095/biolreprod.116.139550.

Li, X., Yao, Y., Wang, J., Shen, Z., Jiang, Z., Xu, S., 2022. Eucalyptol relieves imidacloprid-induced autophagy through the miR-451/Cab39/AMPK axis in Ctenopharyngodon idellus kidney cells. Aquat. Toxicol. 249, 106204 https://doi.org/10.1016/j.aquatox.2022.106204.

Li, Y., Hu, Y., Dong, C., Lu, H., Zhang, C., Hu, Q., Li, S., Qin, H., Li, Z., Wang, Y., 2016. Vimentin-mediated steroidogenesis induced by phthalate esters: involvement of DNA demethylation and nuclear factor κB. PLoS One 11, e0146138. https://doi.org/10.1371/journal.pone.0146138.

Lonare, M., Kumar, M., Raut, S., More, A., Doltade, S., Badgujar, P., Telang, A., 2016. Evaluation of ameliorative effect of curcumin on imidacloprid-induced male reproductive toxicity in wistar rats. Environ. Toxicol. 31, 1250–1263. https://doi.org/10.1002/tox.22132.

Maiuri, M.C., Zalckvar, E., Kimchi, A., Kroemer, G., 2007. Self-eating and self-killing: crosstalk between autophagy and apoptosis. Nat. Rev. Mol. Cell Biol. 8, 741–752. https://doi.org/10.1038/nrm2239.

Mann, U., Shiff, B., Patel, P., 2020. Reasons for worldwide decline in male fertility. Curr. Opin. Urol. 30, 296–301. https://doi.org/10.1097/mou.0000000000000745.

Mendy, A., Pinney, S.M., 2022. Exposure to neonicotinoids and serum testosterone in men, women, and children. Environ. Toxicol. 37, 1521–1528. https://doi.org/10.1002/tox.23503.

Miao, Z., Miao, Z., Wang, S., Wu, H., Xu, S., 2022. Exposure to imidacloprid induce oxidative stress, mitochondrial dysfunction, inflammation, apoptosis and mitophagy via NF-kappaB/JNK pathway in grass carp hepatocytes. Fish. Shellfish Immunol. 120, 674–685. https://doi.org/10.1016/j.fsi.2021.12.017.

Millot, F., Decors, A., Mastain, O., Quintaine, T., Berny, P., Vey, D., Lasseur, R., Bro, E., 2017. Field evidence of bird poisonings by imidacloprid-treated seeds: a review of incidents reported by the French SAGIR network from 1995 to 2014. Environ. Sci. Pollut. Res. 24, 5469–5485. https://doi.org/10.1007/s11356-016-8272-y.

Morales, P.E., Arias-Durán, C., Ávalos-Guajardo, Y., Aedo, G., Verdejo, H.E., Parra, V., Lavandero, S., 2020. Emerging role of mitophagy in cardiovascular physiology and pathology. Mol. Asp. Med. 71, 100822 https://doi.org/10.1016/j.mam.2019.09.006.

Mosher, D.F., Furcht, L.T., 1981. Fibronectin: review of its structure and possible functions. J. Invest. Dermatol. 77, 175–180. https://doi.org/10.1111/1523-1747.ep12479791.

Mosmann, T., 1983. Rapid colorimetric assay for cellular growth and survival: application to proliferation and cytotoxicity assays. J. Immunol. Methods 65, 55–63.

Najafi, G.R., Razi, M., Houshyar, A., Shah, M.S., Feyzi, S., 2010. The effect of chronic exposure with imidacloprid insecticide on fertility in mature male rats. Int. J. Fertil. Steril. 4, 9–16. https://doi.org/10.22074/ijfs.2010.45815.

Ramírez, A., Bravo, A., Jorcano, J.L., Vidal, M., 1994. Sequences 5′ of the bovine keratin 5 gene direct tissue- and cell-type-specific expression of a lacZ gene in the adult and during development. Differentiation 58, 53–64. https://doi.org/10.1046/j.1432-0436.1994.5810053.x.

Saber, T.M., Arisha, A.H., Abo-Elmaaty, A.M.A., Abdelgawad, F.E., Metwally, M.M.M., Saber, T., Mansour, M.F., 2021. Thymol alleviates imidacloprid-induced testicular toxicity by modulating oxidative stress and expression of steroidogenesis and apoptosis-related genes in adult male rats. Ecotoxicol. Environ. Saf. 221, 112435 https://doi.org/10.1016/j.ecoenv.2021.112435.

Schindelin, J., Arganda-Carreras, I., Frise, E., Kaynig, V., Longair, M., Pietzsch, T., Preibisch, S., Rueden, C., Saalfeld, S., Schmid, B., 2012. Fiji: an open-source platform for biological-image analysis, v1.53t (Version 1.53t). Nat. Methods 9, 676–682. https://doi.org/10.1038/nmeth.2019.

Sewer, M.B., Li, D., 2008. Regulation of steroid hormone biosynthesis by the cytoskeleton. Lipids 43, 1109–1115. https://doi.org/10.1007/s11745-008-3221-2.

Shao, X., Swenson, T.L., Casida, J.E., 2013. Cycloxaprid insecticide: nicotinic acetylcholine receptor binding site and metabolism. J. Agric. Food Chem. 61, 7883–7888. https://doi.org/10.1021/jf4030695.

Simon-Delso, N., Amaral-Rogers, V., Belzunces, L.P., Bonmatin, J.-M., Chagnon, M., Downs, C., Furlan, L., Gibbons, D.W., Giorio, C., Girolami, V., 2015. Systemic insecticides (neonicotinoids and fipronil): trends, uses, mode of action and metabolites. Environ. Sci. Pollut. Res. 22, 5–34. https://doi.org/10.1007/s11356-014-3470-y.

Stocco, D.M., Clark, B.J., 1996. Role of the steroidogenic acute regulatory protein (StAR) in steroidogenesis. Biochem. Pharmacol. 51, 197–205. https://doi.org/10.1016/0006-2952(95)02093-4.

Su, F., Zhang, S., Li, H., Guo, H., 2007. In vitro acute cytotoxicity of neonicotinoid insecticide imidacloprid to gill cell line of flounder Paralichthy olivaceus. Chin. J. Oceanol. Limnol. 25, 209–214. https://doi.org/10.1007/s00343-007-0209-3.

Tišler, T., Jemec, A., Mozetič, B., Trebše, P., 2009. Hazard identification of imidacloprid to aquatic environment. Chemosphere 76, 907–914. https://doi.org/10.1016/j.chemosphere.2009.05.002.

Tiwari, A., Kumar, R., Ram, J., Sharma, M., Luthra-Guptasarma, M., 2016. Control of fibrotic changes through the synergistic effects of anti-fibronectin antibody and an RGDS-tagged form of the same antibody. Sci. Rep. 6, 1–13. https://doi.org/10.1038/srep30872.

Tomizawa, M., Casida, J.E., 2005. Neonicotinoid insecticide toxicology: mechanisms of selective action. Annu. Rev. Pharmacol. Toxicol. 45, 247–268. https://doi.org/10.1146/annurev.pharmtox.45.120403.095930.

Tong, N., Witherspoon, L., Dunne, C., Flannigan, R., 2022. Global decline of male fertility: Fact or fiction. B. C. Med. J. 64, 126–130.

Vakifahmetoglu-Norberg, H., Ouchida, A.T., Norberg, E., 2017. The role of mitochondria in metabolism and cell death. Biochem. Biophys. Res. Commun. 482, 426–431. https://doi.org/10.1016/j.bbrc.2016.11.088.

Wu, Z., Zhang, C., 2022. Role of the cytoskeleton in steroidogenesis. Endocr. Metab. Immune Disord. Drug. 22, 549–557. https://doi.org/10.2174/1871530321666211119143653.

Xiong, X., Wu, Q., Zhang, L., Gao, S., Li, R., Han, L., Fan, M., Wang, M., Liu, L., Wang, X., 2022. Chronic stress inhibits testosterone synthesis in Leydig cells through mitochondrial damage via Atp5a1. J. Cell. Mol. Med. 26, 354–363. https://doi.org/10.1111/jcmm.17085.

Xu, H., Ren, D., 2015. Lysosomal physiology. Annu. Rev. Physiol. 77, 57–80. https://doi.org/10.1146/annurev-physiol-021014-071649.
Xu, X., Wang, X., Yang, Y., Ares, I., Martínez, M., Lopez-Torres, B., Martínez-Larrañaga, M.-R., Wang, X., Anadón, A., Martinez, M.-A., 2022. Neonicotinoids: mechanisms of systemic toxicity based on oxidative stress-mitochondrial damage. Arch. Toxicol. 96, 1493–1520. https://doi.org/10.1007/s00204-022-03267-5.
Zhang, S., Peng, X., Yang, S., Li, X., Huang, M., Wei, S., Liu, J., He, G., Zheng, H., Yang, L., Li, H., Fan, Q., 2022a. The regulation, function, and role of lipophagy, a form of selective autophagy, in metabolic disorders. Cell Death Dis. 13, 132. https://doi.org/10.1038/s41419-022-04593-3.
Zhang, W., Huang, T., Sun, Z., Kuang, H., Yuan, Y., Zou, W., Liu, F., Zhang, F., Yang, B., Wu, L., Zhang, D., 2022b. Bisphenol S exposure induces cytotoxicity in mouse Leydig cells. Food Chem. Toxicol. 160, 112805 https://doi.org/10.1016/j.fct.2021.112805.
Zhao, G.-P., Li, J.-W., Yang, F.-W., Yin, X.-F., Ren, F.-Z., Fang, B., Pang, G.-F., 2021. Spermiogenesis toxicity of imidacloprid in rats, possible role of CYP3A4. Chemosphere 282, 131120. https://doi.org/10.1016/j.chemosphere.2021.131120.
Zirkin, B.R., Papadopoulos, V., 2018. Leydig cells: formation, function, and regulation. Biol. Reprod. 99, 101–111. https://doi.org/10.1093/biolre/ioy059.